ELSEVIER

1 June 1999

Optics Communications 164 (1999) 129–136

OPTICS COMMUNICATIONS

www.elsevier.com/locate/optcom

Full length article

Observation of laser-jitter-enhanced hyperfine spectroscopy and two-photon spectral hole-burning

B.S. Ham [a,*], P.R. Hemmer [b], M.S. Shahriar [a]

[a] *Research Laboratory of Electronics, Massachusetts Institute of Technology, Cambridge, MA 02139, USA*
[b] *Air Force Research Laboratory, Hanscom AFB, MA 01731, USA*

Received 6 January 1999; received in revised form 11 March 1999; accepted 17 March 1999

Abstract

We have observed laser-jitter-enhanced high-resolution spectra of three hyperfine states in the ground level ($^3H_4$) of Pr^{3+}:Y_2SiO_5 using coherent population trapping and phase-correlated four-wave mixing. We have also observed optical Raman pulse excited two-photon spectral hole-burning. The observed high-resolution spectra are due to a laser-jitter-suppressed Raman coherence window in an inhomogeneously broadened solid system, and the observed two-photon spectral hole-burning has potential to increase data capacity in Raman excited optical memory (Opt. Lett. 22 (1997) 1849).

PACS: 42.50.Md; 42.65.Hw; 78.47.+p
Keywords: Optical transient phenomena; Free induction decay; Four-wave mixing; Time-resolved optical spectroscopy in condensed matter

1. Introduction

In saturation laser spectroscopy, using narrow bandwidth lasers is generally a big advantage for higher frequency resolution. Therefore, there have been many efforts to develop narrow-bandwidth laser sources. In a three-level energy system, however, two-photon coherence can alleviate such laser bandwidth dependence on spectroscopic resolution, because the two-photon coherence spectral width can be much narrower than each laser linewidth. Recently demonstrated coherent Raman beat in a Λ-system [1] and phase-correlated four-wave mixing in a V-system [2] used weak power dichromatic lasers and showed high-resolution spectroscopy for hyperfine states of inhomogeneously broadened systems. Especially, the phase-correlated four-wave mixing technique in Ref. [2] demonstrated that the spectroscopic resolution for hyperfine structures of an excited state is much higher than that by rf-optical double resonance technique [3].

In this communication, we report laser-jitter-enhanced spectroscopy for hyperfine structures of the ground state of Pr^{3+}-doped Y_2SiO_5 (Pr:YSO) using coherent population trapping (CPT) [4,5] or electromagnetically induced transparency (EIT) [6,7] in the context of an optically thick medium. We also report two-photon spectral hole-burning in an inhomogeneously broadened system of Pr:YSO. As we demonstrated already [8], efficient Raman coherence detec-

* Corresponding author. 716 Princeton Blvd. #19 Lowell, MA 01851, USA. Tel.: +1-781-377-5170; Fax: +1-781-377-2836; E-mail: bham@mit.edu

0030-4018/99/$ - see front matter
PII: S0030-4018(99)00155-8

tion can be accomplished via four-wave mixing processes based on EIT. Here, it should be noted that optical non-linear susceptibility Re[$\chi^{(3)}$] is enhanced while linear susceptibility Im[$\chi^{(1)}$] is suppressed, when EIT is satisfied [9]. This is how four-wave mixing signals are enhanced in an optically thick medium.

For the present study, we apply a time-resolved four-wave mixing technique for the hyperfine spectroscopy. Although, laser-jitter-independent resolution spectroscopy was demonstrated in Ref. [2], this technique should be limited to instantaneous probe interaction as mentioned by the authors. However, the present study is based on CPT or EIT, so the probe field can either be pulsed or cw (see Ref. [8]). Moreover, we observed that the four-wave mixing signal intensity was nearly unaffected by the laser jitter, and the spectroscopic resolution was enhanced with broader laser bandwidth, even though the laser jitter should degrade EIT efficiency in a Λ-system [10]. By comparing our experimental data with numerical calculations, we demonstrate that off-resonant atoms in an inhomogeneous broadened system should contribute to line narrowing of Raman coherence spectral width. For the study of two-photon spectral hole-burning, we measured spin free-induction-decay (FID) signals for all three hyperfine transitions of the ground state ($^3H_4$). The observed FID spectral widths are much narrower than the spin inhomogeneous widths measured by the rf-double resonance technique.

2. Experimental set-up

Fig. 1(a) shows an energy level diagram of Pr:YSO. Our system consists of 0.05 at.% Pr^{3+}-doped Y_2SiO_5. For this work, the relevant optical transition is $^3H_4 \rightarrow {}^1D_2$, and the resonant frequency is 606 nm. The measured absorption coefficient α for that transition is 10 cm^{-1}. The inhomogeneous width for the optical transitions is ~ 4 GHz at liquid helium temperatures, which is much wider than the hyperfine splittings of $^3H_4$. We observed that the optical homogeneous width increases exponentially as temperature increases from 4 K to 6 K in Pr:YSO, while the spin homogeneous width is almost constant

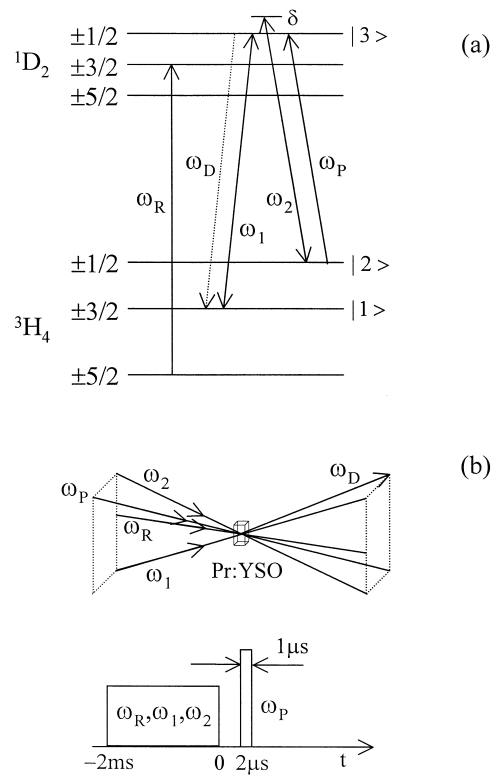

Fig. 1. (a) Energy level diagram of Pr:YSO and (b) laser beam propagation scheme and pulse sequence for phase-correlated four-wave mixing spectroscopy.

[11]. Each ground ($^3H_4$) and excited ($^1D_2$) state has three doubly degenerate hyperfine states. The splittings between the hyperfine states of the ground level $^3H_4$ are 10.2 MHz ($\pm 1/2 \leftrightarrow \pm 3/2$), 17.3 MHz ($\pm 3/2 \leftrightarrow \pm 5/2$), and 27.5 MHz ($\pm 1/2 \leftrightarrow \pm 5/2$) [12]. The ground state population decay time T_1 is ~ 100 s [12], and the spin transverse decay time T_2 for the 10.2 MHz transition is 500 μs at 6 K [11]. Due to the long population decay time on the hyperfine states of the ground level, optical spectral hole-burning persists unless the populations are redistributed among the three hyperfine states.

The laser fields of ω_1 and ω_2 in Fig. 1(a) are for Raman pump pulses that create two-photon coherence through CPT or EIT. Here, it should be noted that the pump Rabi frequency Ω does not have to be strong to reach near maximal coherence because the Raman coherence amplitude depends on the pulse area Θ: $\Theta = \int_0^t \Omega(t')\mathrm{d}t'$ [13]. However, in an opti-

cally thick medium, a strong Rabi frequency is necessary and a benefit for strong four-wave mixing signal due to EIT effects. For resonant Raman transition, the difference frequency of the pump beams ω_1 and ω_2 should match the hyperfine splitting, and each optical frequency should be resonant to its transition. Laser field ω_P acts as a probe (read) beam, which scatters off on the two-photon coherence phase gratings created by the pump beams and generates the four-wave mixing signal ω_D that satisfies phase matching condition $k_D = k_1 - k_2 + k_P$. Repump field ω_R is used to provide spectral selection in the otherwise inhomogeneously broadened system (~ 4 GHz inhomogeneous width). Non-collinear propagation scheme has an advantage of background-free detection of the four-wave mixing signal (Fig. 1(b)).

Fig. 1(b) shows a schematic of the experimental set-up for Raman coherence spectroscopy using phase-correlated four-wave mixing. We use acousto-optic modulators driven by frequency synthesizers (PTS 160) to generate four different coherent laser frequencies as shown. All laser beams are circularly polarized and focused into the sample by a 30-cm focal length lens, and the focused beam diameter (e^{-1} in intensity) is ~ 100 μm. The power of the pump lasers ω_1 and ω_2 is 18 mW and 21 mW, respectively. The power of the probe and repump lasers ω_P and ω_R is 22 mW and 12 mW, respectively. To generate laser pulses, we use rf switches driven by pulse generators. The probe pulse width is fixed at 1 μs and is delayed by 2 μs at the end of the pump pulses. A Boxcar collects 30 samples of the four-wave mixing signal ω_D. The pulse repetition rate is low enough (30 Hz) so that the Raman coherence cannot be accumulated. The angle between the pump beams is about ~ 100 mrad. The persistent spectral hole-burning crystal of Pr:YSO is inside a cryostat at a temperature of 6 K. The size of the crystal is 3.5 mm × 4 mm × 3 mm, and optical *B*-axis is along the 3-mm length. The laser propagation direction is almost parallel to the optical axis.

3. Results and discussion

Fig. 2 shows the four-wave mixing signals ω_D vs. detuning δ of the pump beam ω_2. The Raman pulse width is fixed at 2 ms. For Fig. 2(a), we used an unstabilized laser whose jitter is ~ 80 MHz. The measured laser jitter was dominated by low frequencies less than 50 kHz. The width (FWHM) of the diffracted beam ω_D in Fig. 2(a) is 53.7 kHz. In Fig. 2(b), we stabilized the lasers by using an external Fabry–Perot cavity. The frequency-stabilized laser jitter is 1–2 MHz. The width (FWHM) of the ω_D in Fig. 2(b) is 77.6 kHz, which is widened by a factor of 1.4. Here, it should be noted that both spectral widths in Fig. 2 are power broadened. In Fig. 2(b), the function of the repump ω_P is critical to the four-wave mixing signal intensity due to the persistent spectral hole-burning and narrower laser bandwidth. However, in Fig. 2(a), we observed that the repump gives little effect on the four-wave mixing signal intensity because the laser jitter is much wider than the hyperfine splittings, so the repump does not function to the spectral selectivity.

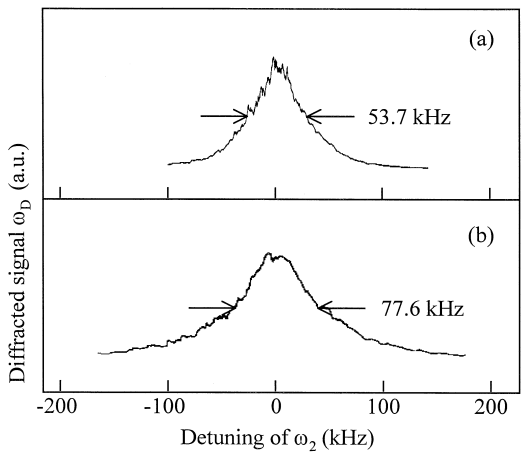

Fig. 2. Four-wave mixing signal ω_D vs. two-photon detuning δ with (a) unstablized and (b) stabilized lasers.

To analyze the experimental data in Fig. 2, we numerically solved density matrix equations for 2 ms Raman pulse as a function of two-photon detuning δ. The four-wave mixing signal intensity I_D is proportional to the product of square of the Raman coherence $\mathrm{Re}(\rho_{12})$ and the probe intensity I_P: $I_D \propto \mathrm{Re}(\rho_{12})^2 I_P$. The fact of $I_D \propto \mathrm{Re}(\rho_{12})^2 I_P$ has been experimentally demonstrated [14]. Fig. 3 shows $\mathrm{Re}(\rho_{12})$ vs. detuning δ of ω_2 for three different cases of laser jitter. For the calculations, we assumed a closed three-level system and used experimental values for the parameters. Each pump Rabi fre-

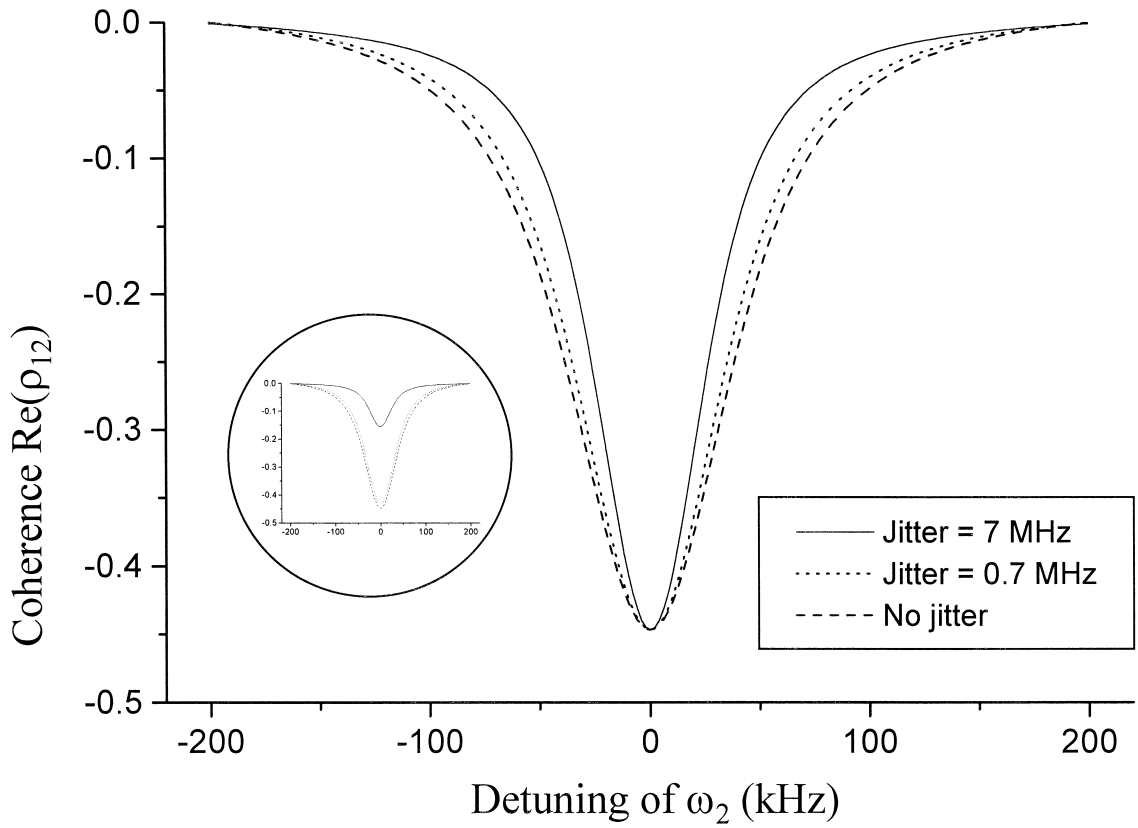

Fig. 3. Numerical simulations for the Raman excited spin coherence Re(ρ_{12}) vs. two-photon detuning δ; optical population (coherence) decay rate is 1 kHz (20 kHz) for each transition. The decay rates for hyperfine transitions are assumed to be zero. Rabi frequency of ω_1 (ω_2) is 200 kHz (200 kHz). The inhomogeneous width for the transition $|1\rangle \leftrightarrow |2\rangle$ is 29 kHz. Each laser jitter is assumed to be Gaussian. Inset: actual data.

quency Ω_i ($i = 1$ or 2) is estimated at 200 kHz. Here, laser jitter should determine the spectral width of effective atoms due to the persistent spectral hole-burning. We assumed that the laser jitter is Gaussian. The total number of atoms, however, is fixed to be the same for all three cases (see the inset). For the calculation, we divided the spectral width of the atoms into many subsets and solved 9×9 density matrix equations for each set of atoms individually as functions of two-photon detuning δ and spin detuning (in the hyperfine inhomogeneous width). The spectral width of each set of atoms is chosen to be less than the pump Rabi frequency. Fig. 3 is the sum of Re(ρ_{12}) for all the sets of atoms as a function of two-photon detuning. To compare spectral widths of Re(ρ_{12}) with one another, the plots in Fig. 3 are normalized. For this, the dashed curve with no laser jitter is chosen as a reference, and the number of atoms for the solid (dotted) curve is increased by a factor of 2.89 (1.04). As seen in Fig. 3, the spectral width of the coherence Re(ρ_{12}) becomes narrower as the laser jitter increases.

Fig. 4 shows Raman coherence Re(ρ_{12}) as both functions of two-photon detuning and the detuning of individual atoms in the inhomogeneous line from the optical resonance for the case of 7 MHz laser jitter in Fig. 3. As seen in Fig. 4, off-resonance atoms contribute to the line-narrowing of Re(ρ_{12}). Here, it should be noted that the off-resonance atoms should produce lower Raman coherence, too. If the same number of atoms is considered, overall four-wave mixing signal should be degraded as jitter

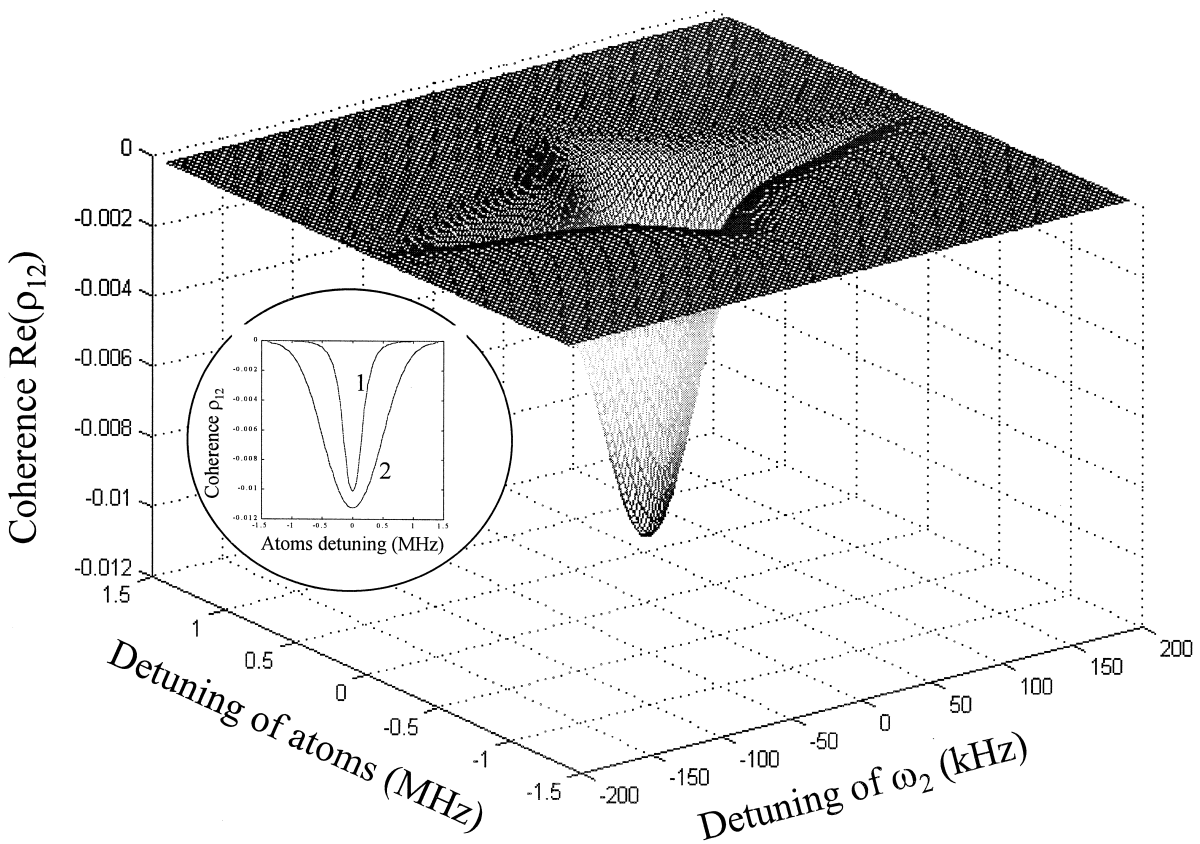

Fig. 4. Numerical simulation for the Raman excited spin coherence Re(ρ_{12}) vs. atoms detuning and two-photon detuning δ for solid curve in Fig. 3. Inset: Re(ρ_{12}) vs. atoms detuning for zero detuning of ω_2, and $\Omega_2 = 5\Omega_1$, where Ω_i is Rabi frequency of curve *i*.

increases as shown in the inset of Fig. 3. However, in an inhomogeneously broadened persistent spectral hole-burning system, the total number of active atoms is determined by the spectral selection determined by the laser jitter. It also depends on pump Rabi frequency. To see how pump Rabi frequency modifies the atoms distribution (inhomogeneous width), we examine it in the inset of Fig. 4. The inset shows coherence Re(ρ_{12}) vs. atoms detuning from the center for zero detuning of ω_2. The Rabi frequency of the curve '1' ('2') is 200 (1000) kHz. As seen in the inset of Fig. 4, bigger Rabi frequency excites more atoms and generates stronger Raman coherence Re(ρ_{12}), and Re(ρ_{12}) becomes weaker for the atoms detuned more. Therefore, broader laser jitter should suppress Raman coherence spectral width while keeping or enhancing overall four-wave mixing intensity due to the increasing number of interacting atoms in an inhomogeneously broadened persistent-spectral hole-burning medium.

In Fig. 5(a), we varied the Raman pulse width and measured the spectral width of each four-wave mixing signal as we did in Fig. 2. The spectral width of the four-wave mixing signal ω_D in Fig. 5(a) reaches minimum as the Raman pulse width lengthens. This is additional evidence of laser-jitter-suppressed Raman coherence as discussed in Figs. 2–4. Obviously, shorter pulse has narrower jitter, because the jitter is dominated by low frequencies (less than 50 kHz) as mentioned above. In Fig. 5(a), for short pulses less than 1 ms, however, the four-wave mixing signals are spectrally broadened for both cases. The line-broadening in this short pulse region is due to the increasing Fourier transform width.

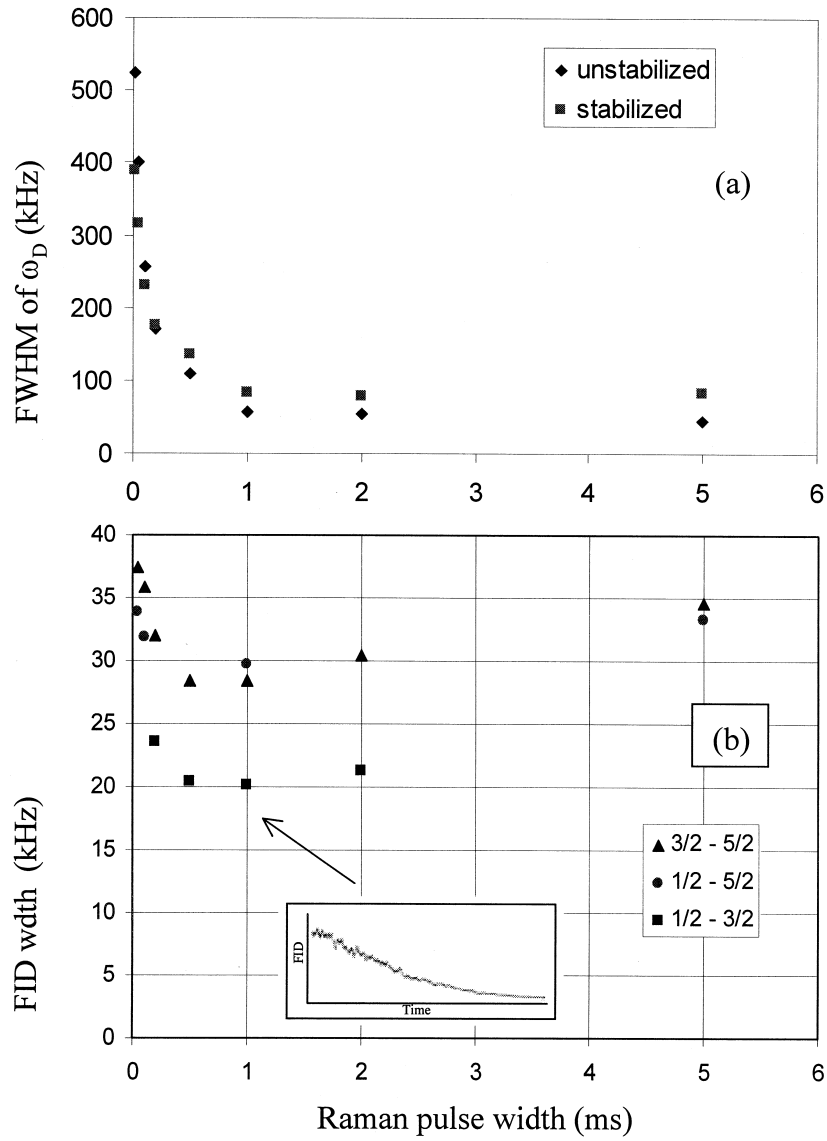

Fig. 5. Spectral widths of (a) four-wave mixing signal ω_D and (b) Raman pulse excited spin FID vs. Raman pulse width.

In Fig. 5(b), we show the Raman optical pulse excited spin spectral holes. For FID signals, the probe was scanned from 2 μs to 20 μs. The inset shows a data of FID signals for 1 ms pump pulse. To determine the FID spectral width Δ, we measured decay time τ when the FID signal intensity drops by a factor of $\exp(-2)$; $\Delta = 1/(\pi\tau)$. Here, the factor 2 comes from the intensity measurement (intensity $\propto$ $|\text{amplitude}|^2$). Unlike the spectral width of the four-wave mixing signals in Fig. 5(a), we observed sub-inhomogeneous widths for the hyperfine transitions. The measured spin inhomogeneous widths by the rf-optical double resonance are 29 kHz for the transition $|1\rangle \leftrightarrow |2\rangle$ and ~ 70 kHz for the transitions $|0\rangle \leftrightarrow |2\rangle$ and $|0\rangle \leftrightarrow |1\rangle$. The sub-inhomogeneous width is the evidence of the spin spectral holes burned by the Raman optical fields via two-photon coherence. The observed two-photon spectral hole-

burning phenomenon has potential for increasing storage capacity in Raman excited spin echo memory [11].

To support the observed sub-inhomogeneous widths of FID signals in Fig. 5(b), we numerically calculated it for a 1 ms Raman pulse. Fig. 6 shows Raman coherence Re(ρ_{12}) vs. spin detuning in the inhomogenously broadened hyperfine transition. The excited spins only contribute to the FID signals, because four-wave mixing generation is based on the Raman coherence Re(ρ_{12}) as we discussed in Fig. 3. Fig. 6(a) shows Raman coherence ρ_{12} vs. spin detuning for 10 different Raman Rabi frequencies Ωs ($\Omega^2 = \Omega_1^2 + \Omega_2^2$). As the Rabi frequency increases, the two-photon excited spin spectral width becomes saturated; the inhomogeneous width is assumed Gaussian. Unlike one-photon excitation in a two-level system, however, the excited spin spectral width can be less than the inhomogeneous width (29 kHz), even if the Rabi frequency Ω is much bigger than

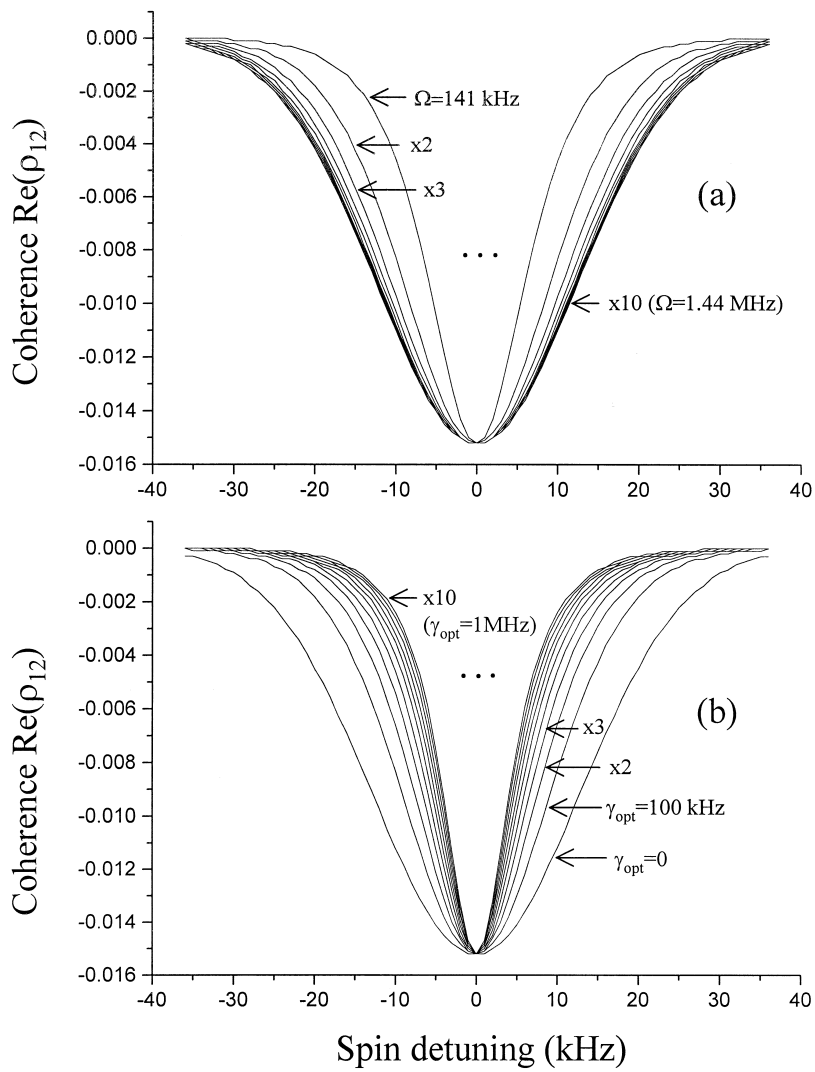

Fig. 6. Numerical simulation for the Raman excited spin coherence Re(ρ_{12}) vs. spin distribution. Optical transition is assumed to be homogeneously broadened. (a) Optical homogeneous decay rate γ_{opt} = 100 kHz and (b) $\Omega_1 = \Omega_2$ = 200 kHz.

this width. For $\Omega = 283$ kHz, we found that Raman excited spin spectral width is ~ 21 kHz. This is similar to the experimental result observed in Fig. 5(b).

Fig. 6(b) shows Raman coherence ρ_{12} vs. spin detuning with the optical homogeneous decay rate γ_{opt} as a free parameter and $\Omega = 283$ kHz. As we mentioned above that CPT or EIT is inversely proportional to γ_{opt}, the excited spin width is also inversely proportional to γ_{opt}. Therefore, the FID width can be narrower than the inhomogeneous width even if the optical Rabi frequency is larger than the inhomogeneous width. This is because the two-photon coherence creating rate becomes slower as two-photon detuning (spin detuning) is made larger.

4. Conclusion

In conclusion, we demonstrated laser-jitter-enhanced high-resolution spectroscopy for hyperfine structures in the ground state of Pr:YSO using resonant Raman pulses and phase-correlated four-wave mixing. We also observed two-photon coherence excited spin spectral holes. The observed laser-jitter-enhanced resolution has potential applications to high-resolution spectroscopy especially with unstabilized lasers. The observed two-photon spectral hole-burning is important for further study of Raman excited optical memory and quantum optics involving spin transitions.

Acknowledgements

We acknowledge that this research was supported by Air Force Research Laboratory (Grant No. F30602-96-2-0100) and U.S. Air Force Office of Scientific Research (Grant No. F49620-96-1-0395).

References

[1] T. Blasberg, D. Suter, Bichromatic excitation of coherent Raman beats in rare-earth solids, Phys. Rev. B 51 (1995) 6309.
[2] Y.S. Bai, R. Kachru, High-resolution spectroscopy of hyperfine structure using phase-correlated four-wave mixing, Phys. Rev. Lett. 67 (1991) 1859.
[3] L.E. Erickson, The nuclear quadrupole interaction in Pr^{3+}:LaF_3—an optical-rf double resonance measurement of the ground electronic state, Opt. Commun. 21 (1977) 147.
[4] G. Alzetta, A. Gozzini, L. Moi, G. Orriols, An experimental method for the observation of rf transitions and laser beat resonances in oriented Na vapor, Nuovo Cimento B 36 (1976) 5.
[5] H.R. Gray, R.M. Whitley, C.R. Stroud Jr., Coherent trapping of atomic populations, Opt. Lett. 3 (1979) 218.
[6] S.E. Harris, Electromagnetically induced transparency, Physics Today 50 (7) (1997) 36, and references therein.
[7] B.S. Ham et al., Efficient electromagnetically induced transparency in a rare-earth doped crystal, Opt. Commun. 144 (1997) 227, For EIT in solids.
[8] B.S. Ham, M.S. Shahriar, P.R. Hemmer, Enhanced nondegenerate four-wave mixing owing to electromagnetically induced transparency in a spectral hole-burning crystal, Opt. Lett. 22 (1997) 1138.
[9] S.E. Harris, J.E. Field, A. Imamoglu, Nonlinear optical processes using electromagnetically induced transparency, Phys. Rev. Lett. 64 (1990) 1107.
[10] Y.-Q. Li, M. Xiao, Observation of quantum interference between dressed states in an electromagnetically induced transparency, Phys. Rev. A 51 (1995) 4959.
[11] B.S. Ham, M.S. Shahriar, M.K. Kim, P.R. Hemmer, Frequency-selective time-domain optical data storage by electromagnetically induced transparency in a rare-earth doped solid, Opt. Lett. 22 (1997) 1849.
[12] K. Holliday, M. Croci, E. Vauthey, U.P. Wild, Spectral hole burning and holography in an Y_2SiO_5:Pr^{3+} crystal, Phys. Rev. B 47 (1993) 14741.
[13] B.S. Ham, M.S. Shahriar, M.K. Kim, P.R. Hemmer, Spin coherence excitation and rephasing via optically shelved atoms, Phys. Rev. B 58 (1998) R11825.
[14] S. Babin, U. Hinze, E. Tiemann, B. Wellegehausen, Continuous resonant four-wave mixing in double-Λ level configuration of Na_2, Opt. Lett. 21 (1996) 1186.